Rotor Fault Analysis in a Doubly-Fed Induction Generator Using Impedance Matrix Technique.

D.G. Dorrell[1], A. Salah[2] and Y. Guo[2]

1. Department of Electrical, Electronics and Computer Engineering, University of KwaZulu-Natal, Durban, South Africa; 2. School of Electrical Engineering, University of Technology Sydney, Sydney, Australia

Introduction Condition monitoring is a standard method for scheduling maintenance and ensuring that catastrophic failures do not occur in industrial motors. It is used in various applications where there is high capital cost or the location is remote. Condition monitoring is increasingly used in renewable energy. Different methods for fault identification have been developed and used effectively to detect machine faults at different stages using parameters such as current, voltage, speed, torque, noise and vibrations [1]-[4]. In most cases, faults produce one or more indicative signs, such as increased losses, excessive heating, torque pulsation, and unbalanced air-gap voltages and line currents. The faults in [5] where 41 % are bearing faults, 37 % are stator faults, 10 % are rotor faults and 12 % are others. [6][7] show techniques for analysing asymmetrical wound rotor machines using simple positive and negative equivalent circuits for a machine with unbalanced impedance in the secondary circuit. Stator current monitoring is another popular method where signature currents are monitored [8]. Vibration signal analysis has been widely used in the fault detection of induction machines. Faults create harmonics with different frequencies and power levels in the vibration signal and are sensed via a vibration sensor mounted on the stator frame. The spectrum is calculated using a fast Fourier transform (FFT). These methods should be able to expose faults and to prevent the total damage and unexpected shutdowns. This work develops a steady-state analysis of a wound rotor induction machine capable of including rotor asymmetry; the field analysis is applied to a doubly-fed induction generator (DFIG) with general external impedance asymmetry. The measured and predicted values for torque, current, and power losses will be used to verify the technique. The simulation of an unbalanced rotor was done by connected the rotor with external resistances. Determining the currents flowing in the various stator and rotor windings is the first necessary to evaluate rotor symmetry or asymmetry. By the coupling impedance method described in [9], this can be done. The machine analysis resolves the airgap flux into a harmonic series of traveling waves with different pole numbers rotating in either direction. The authors have put the primary results in [10] and the rest of the experiment work results will be put forward here. **Matrix Equations** The main advantage of the method, that any asymmetrical winding can be considered. In addition to this, the electric field in the airgap can be derived and the EMF induced into any winding calculated, leading to expressions for the coupling impedances between the various machine windings. These can be expressed as an impedance matrix. The machine currents in (1), Fig. 1, are obtained from knowledge of the applied voltages when the matrix is solved. It can be developed to incorporate eccentricity faults for condition monitoring of wound rotor machines [11]. The impedance matrix includes the impedances for the stator and rotor which are functions of the three-phase windings on the stator and rotor, assuming the rotor is short-circuited as in (1), Fig. 1. If there is asymmetry, there will be a backwards rotating MMF wave. It subsequently induces EMFs of frequency $(1 - 2s)f_m$ in the stator windings. For that reason, it is necessary to add other components in the impedance matrix to accommodate the $(1 - 2s)f_m$ current components. These components result in torque pulsation at $2sf$. FIg. 1 gives these equations showing the matrix for the additional backwards-rotating component (2), the impedance components (3), the effective current densities on the stator (4), and finally the torque equation. These will be further derived and expained in the paper. This algorithm is implemented on a machine - the basic machine specification is given in Table 1, Fig. 1. **Simulation of Rotor Faults** Tests were done with the rotor short circuited and balanced (healthy). Fig 2(a) gives the current and Fig. 2(b) the torque. The results validate the method. A rotor fault is then put into the rotor using a small resistor (2Ω) in the star-connect rotor via the slip rings. This will cause the stator currents to have two components, whose frequencies are ω_s and $(2s-1)\omega_s$. As the frequencies of these components differ with $2sf_s$, oscillations will be present in the torque as incidated by (5), Fig. 1. Fig. 2(c) shows the steady state torque for the healthy motor, and the motor with an added 2 Ω resistor in the rotor. The machine will operate at a higher slip at full load making it less efficient. In DFIG operation the machine operates at a wide speed range and the torque will vary greatly with asymetrical rotro impedance, including when it is connected to an inverter. Fig. 2(d) shows that I_{sb} falls to zero at the half-speed point. This is where the backwards rotating field component produced by the asymmetrical rotor is stationary with respect to the stator, and can also induce no EMFs in the stator coils. **Conclusions** This digest develops a simple yet powerful model for studying a wound rotor induction machine that can be used for studying the behavior of DFIG machines. The impedance matrix can be improved in order to incorporate eccentricity faults and rotor winding and stator faults. As illustrated here, the impedance method is flexible and powerful and suitable for use as the basis as a condition monitoring system. Preliminary results are put forward here; further analysis and results will be put forward in the full paper.

[1] S. Djurovic, C.J. Crabtree, P.J. Tavner and A.C. Smith, "*Condition monitoring of wind turbine induction generators with rotor electrical asymmetry*," IET Renew. Power Gener., 2012, Vol. 6, Iss. 4, pp. 207–216. [2] Y. Amirat, M. E. H. Benbouzid, B. Bensaker and R. Wamkeue, "*Condition Monitoring and Fault Diagnosis in Wind Energy Conversion Systems*: *A Review,*" IEEE PEMDC conference, Antalya, Turkey, 3-5 May 2007. [3] B. Lu, Y. Li, X. Wu and Z. Yang, "*A Review of Recent Advances in Wind Turbine Condition Monitoring and Fault Diagnosis,*" IEEE PEMWA conference, Lincoln, NE, USA, 24026 June 2009 pp 1-7. [4] W. Yang, P. J. Tavner and M. Wilkinson, *"Wind Turbine Condition Monitoring and Fault Diagnosis Using both Mechanical and Electrical Signatures,*" IEEE/ASME Int. Conf. on Adv. Int. Mech., Xi'an, China, 2-5 July 2008, pp 1296-1301. [5] W. T. Thomson and M. Fenger, "*Current signature analysis to detect induction motor faults*," IEEE Industry Applications Magazine, vol. 7, no. 4, 2001, pp 26- 34. [6] EPRI, "Improved Motors for Utility Applications," EPRI Final Report, 1982. [7] T. Barton and B. Doxey, "*The operation of three-phase induction motors with unsymmetrical impedance in the secondary circuit,*" Proceedings of the IEE-Part A: Power Engineering, vol. 102, pp. 71-79, 1955. [8] D. G. Dorrell, W. T. Thomson and S. Roach, "*Analysis of airgap flux, current and vibration signals as a function of the combination of static and dynamic airgap eccentricity in 3-phase induction motors*", IEEE Transactions on Industry Applications, Vol. 33, No.1, Jan. 1997, pp 24-34. [9] D. G. Dorrell, "Calculation of unbalanced magnetic pull in cage induction machines," Thesis, University of Cambridge, 1993. [10] Ahmad Salah, David Dorrell," *Impedance Matrix Analysis Technique in Wound aimed Rotor Induction Machines Including General Rotor Asymmetry,"* IEEE/IECON. Conf., Florance, italy, 23-27 Oct. 2016. [11] D. G. Dorrell and A. Salah, "Detection of Rotor Eccentricity in Wound Rotor Induction Machines using Pole-Specific Search Coils," IEEE Trans. on Magnetics, Vol. 51, no. 11, Nov, 2015, Article #: 8111604, DOI: 10.1109/TMAG.2015.2443711.

The impedance matrix includes the impedances for the stator and rotor

$$\begin{bmatrix} \bar{v}_s \\ 0 \\ 0 \\ 0 \\ 0 \end{bmatrix} = [\bar{Z}] \begin{bmatrix} \bar{I}_{s_f} \\ \bar{I}_{s_b} \\ \bar{I}^n_{r_1} \\ \bar{I}^n_{r_2} \\ \bar{I}^n_{r_3} \end{bmatrix} = \begin{bmatrix} \bar{Z}_{s,s_f} & 0 & \bar{Z}^n_{s_f,r_1} & \bar{Z}^n_{s_f,r_2} & \bar{Z}^n_{s_f,r_3} \\ 0 & \bar{Z}^n_{s,s_b} & \bar{Z}^n_{s_b,r_1} & \bar{Z}^n_{s_b,r_2} & \bar{Z}^n_{s_b,r_3} \\ \bar{Z}^n_{r_1,s_f} & \bar{Z}^n_{r_1,s_b} & \bar{Z}^n_{r_1,r_1} & \bar{Z}^n_{r_1,r_2} & \bar{Z}^n_{r_1,r_3} \\ \bar{Z}^n_{r_2,s_f} & \bar{Z}^n_{r_2,s_b} & \bar{Z}^n_{r_2,r_1} & \bar{Z}^n_{r_2,r_2} & \bar{Z}^n_{r_2,r_3} \\ \bar{Z}^n_{r_3,s_f} & \bar{Z}^n_{r_3,s_b} & \bar{Z}^n_{r_3,r_1} & \bar{Z}^n_{r_3,r_2} & \bar{Z}^n_{r_3,r_3} \end{bmatrix} \begin{bmatrix} \bar{I}_{s_f} \\ \bar{I}_{s_b} \\ \bar{I}^n_{r_1} \\ \bar{I}^n_{r_2} \\ \bar{I}^n_{r_3} \end{bmatrix} \quad (1)$$

This can be further developed to include rotor voltages for a DFIG control:

$$\begin{bmatrix} \bar{v}_s \\ 0 \\ \bar{v}_{r1} \\ \bar{v}_{r2} \\ \bar{v}_{r3} \end{bmatrix} = \begin{bmatrix} \bar{Z}_{s,s_f} & 0 & \bar{Z}^n_{s_f,r_1} & \bar{Z}^n_{s_f,r_2} & \bar{Z}^n_{s_f,r_3} \\ 0 & \bar{Z}^{n/}_{s,s_b} & \bar{Z}^n_{s_b,r_1} & \bar{Z}^n_{s_b,r_2} & \bar{Z}^n_{s_b,r_3} \\ \bar{Z}^n_{r_1,s_f} & \bar{Z}^n_{r_1,s_b} & \bar{Z}^{n/}_{r_1,r_1} & \bar{Z}^n_{r_1,r_2} & \bar{Z}^n_{r_1,r_3} \\ \bar{Z}^n_{r_2,s_f} & \bar{Z}^n_{r_2,s_b} & \bar{Z}^n_{r_2,r_1} & \bar{Z}^{n/}_{r_2,r_2} & \bar{Z}^n_{r_2,r_3} \\ \bar{Z}^n_{r_3,s_f} & \bar{Z}^n_{r_3,s_b} & \bar{Z}^n_{r_3,r_1} & \bar{Z}^n_{r_3,r_2} & \bar{Z}^{n/}_{r_3,r_3} \end{bmatrix} \begin{bmatrix} \bar{I}_{s_f} \\ \bar{I}_{s_b} \\ \bar{I}^n_{r_1} \\ \bar{I}^n_{r_2} \\ \bar{I}^n_{r_3} \end{bmatrix} \quad (2)$$

where

$$\bar{Z}^{n/}_{s,s_b} = \bar{Z}^n_{s,s_b} + Z_{ex,S}\ ,\ \bar{Z}^{n/}_{r_1,r_1} = \bar{Z}^n_{r_1,r_1} + Z_{ex,r1}$$

$$\bar{Z}^{n/}_{r_2,r_2} = \bar{Z}^n_{r_2,r_2} + Z_{ex,r2}\ \text{, and}\ \bar{Z}^{n/}_{r_3,r_3} = \bar{Z}^n_{r_3,r_3} + Z_{ex,r3} \quad (3)$$

The stator MMF waves are given below for an unbalanced current set

$$\bar{J}^n_{st_f} = \bar{N}^{n*}_{st}\left(\bar{I}_{sa} + a^{1-n}\bar{I}_{sb} + a^{n-1}\bar{I}_{sc}\right)$$

$$\bar{J}^n_{st_b} = \bar{N}^{n*}_{st}\left(\bar{I}_{sa} + a^{n-1}\bar{I}_{sb} + a^{1-n}\bar{I}_{sc}\right) \quad (4)$$

The torque, in general form is then

$$T = \frac{2\pi r^2 \mu_o L_{st}}{p_m g}\mathrm{Re}\left\{j\left(\bar{J}_{st_b}\bar{J}_{r_b}{}^* - \bar{J}_{st_f}\bar{J}_{r_f}{}^*\right) + j\left(\bar{J}_{st_b}\bar{J}_{r_f} - \bar{J}_{st_f}\bar{J}_{r_b}\right)e^{j2s\omega t}\right\} \quad (5)$$

Table 1. MACHINE SPECIFICATION

Name plate details	
Power [HP]	10 (or 7.46 kW)
Speed [rpm]	1420
Frequency [Hz]	50
Stator voltage [V]	400/440 Delta
Stator rated current [A]	13
Rotor Voltage [V]	200
Rated rotor current [A]	22
Number of Poles	4
Slip [p.u.]	0.0533

Fig. 1

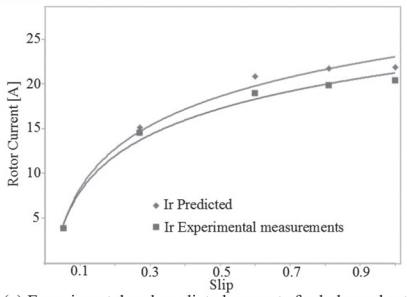

(a) Experimental and predicted currents for balanced rotor

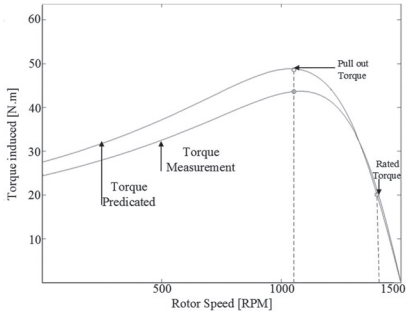

(b) Experimental and predicted torques for balanced rotor

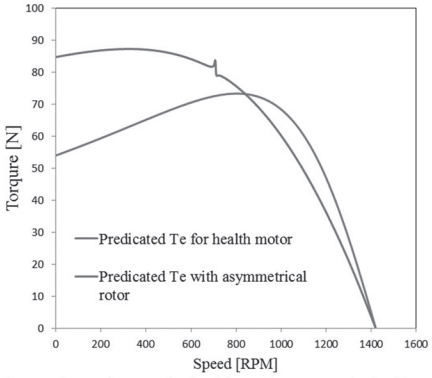

(c) Comparison of torque for healthy and asymmetrical with speed

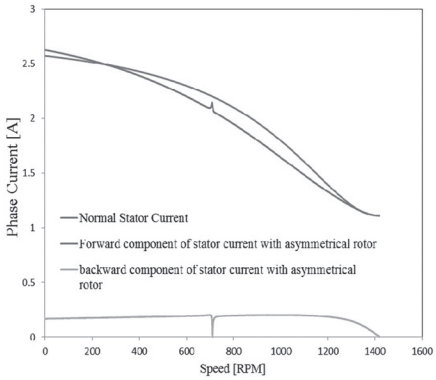

(d) Comparison of currents for healthy and asymmetrical with speed, including the backwards component of current

Fig. 2